Materials Science & Engineering A 908 (2024) 146726

Contents lists available at ScienceDirect

Materials Science & Engineering A

journal homepage: www.elsevier.com/locate/msea

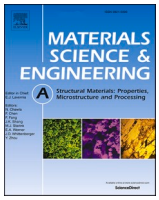

Gaining understanding of the effect of alloy composition on the properties of Ti–Cu–Mn–Al alloys

M. Al-hajiri [a], Y. Alshammari [a,b], F. Yang [a], L. Bolzoni [a,*]

[a] School of Engineering, The University of Waikato, Hamilton, 3240, New Zealand
[b] Construction and Building Materials, Energy and Building Research Centre, Kuwait Institute for Scientific Research, P.O. Box 24885, Safat, 13109, Kuwait

ARTICLE INFO

Keywords:
Titanium alloys
Powder metallurgy
Blended elemental
Homogeneous microstructure
Mechanical properties

ABSTRACT

High performance cheaper Ti alloys can be developed based on the addition of several alloying elements, amongst which are Cu, Mn and Al. Studies are available in literature about binary and some ternary alloys based on the addition of these elements; however, no quaternary Ti–Cu–Mn–Al alloys were developed. Therefore, in this study quaternary Ti–Cu–Mn–Al alloys were manufactured via powder metallurgy to gain a better understanding of the effect of the alloy composition and the achievable mechanical performance. It is found that the selected quaternary Ti–Cu–Mn–Al alloys are characterised by a lamellar structure, which is progressively refined as the amount of alloying elements increases, and precipitation of the Ti_2Cu intermetallic occurs if the Cu content is high enough. The amount of residual porosity increases and changes morphology as more thermal energy is invested in the diffusion of the alloying elements. In terms of mechanical behaviour, the quaternary Ti–Cu–Mn–Al alloys undergo both elastic and plastic deformation upon tensile loading. Strength and hardness linearly increase and the ductility monotonically decreases, which is the result of the compromise between the amount of residual porosity and the several strengthening mechanisms brought about by the actual total amount of alloying elements added.

1. Introduction

Ti and its alloys are commonly used in high demanding industries like the aerospace and the biomedical due to their high cost and balance of properties. The latter include low density, high strength, corrosion resistance, and biocompatibility [1,2]. The effort to reduce the cost of Ti alloys is threefold, including developing new more energy efficient extraction processes, using alternative more economical manufacturing methods (e.g. net shaping), and create new chemical compositions bearing cheap alloying elements. In terms of net shaping, powder metallurgy techniques are ideal to manufacture Ti alloys due to their high materials' yield, reduce power consumption and reactivity by being solid state methods, and limited amount of finishing operations required [3,4]. Regarding new chemical compositions, alloying elements such as Cu, Mn and Al can be considered for a variety of reasons including, respectively, achieving antibacterial properties, enhance biocompatibility, and stabilise the α phase on top of improving the mechanical behaviour. It is worth mentioning that both Cu and Mn are eutectoid β stabilisers whereas Al is a α stabiliser.

Regarding the development of binary Ti–Cu alloys, the arc melting under protective atmosphere casting process has been widely studied. This technique was used by Kikuchi et al. [5] to manufacture Ti-(0.5–10 %)Cu alloys, by Zhang et al. [6] to process the Ti-(5–10 %)Cu alloys, by Yi et al. [7] to obtain Ti-(2–10 %)Cu alloys, and by Zhang et al. [8] to produce Ti-(2–4%)Cu alloys. Characterisation of the cast as well as of some heat treated alloys primarily included microstructure, mechanical properties, and antibacterial behaviour. When it comes to binary Ti–Cu alloys developed by powder metallurgy, vacuum hot pressure sintering has been the dominant technique. This method was used by Zhang et al. [9] to manufacture Ti-(5–10 %)Cu alloys using ball milled high purity powder blends, which were consolidated using the 850–1050 °C sintering temperature range while keeping constant the sintering time at 2 h and the uniaxial pressure at 30 MPa. Some of the vacuum hot pressure sintered samples were also plastically deformed at 800 °C by means of extrusion. Zhang et al. [6] also studied the same alloys vacuum hot pressure sintered at 800 °C for 1 h but without applied pressure whilst Liu et al. [10] used vacuum hot pressure sintering to manufacture Ti-(2–25 %)Cu alloys. Similar properties to those characterised for cast alloys were quantified in the case of powder metallurgy binary Ti–Cu alloys. Major modifications of binary Ti–Cu alloys included the addition

* Corresponding author.
E-mail address: bolzoni.leandro@gmail.com (L. Bolzoni).

https://doi.org/10.1016/j.msea.2024.146726
Received 2 April 2024; Received in revised form 7 May 2024; Accepted 27 May 2024
Available online 31 May 2024

of Fe [11] or Ni [12].

Concerning binary Ti–Mn alloys, casting has also been greatly investigated [13–17] where Kim et al. [17] manufactured Ti-(5–20 %) Mn alloys starting from Ti sponge and Mn ingots which were remelted several times before being subjected to a heat treated for 4 h below the solidus temperatures to achieve better performance (i.e. hardness, oxidation resistance, and corrosion resistance) with respect to Ti. Similarly, Gouda et al. [13] produced Ti-(8–20 %)Mn alloys from a mixture of Ti sponge and Mn flakes and the cast alloys were eventually solution treated achieving an improvement of the cold workability with the Mn content. In the case of powder metallurgy binary Ti–Mn alloys, Fernandes Santos et al. [18] manufactured Ti-(8–17 %)Mn alloys by means of metal injection moulding for shaping followed by vacuum sintering at 1100 °C for 8 h as well as a solution treatment at 900 °C for 1 resulting in the increase of the hardness and the loss of tensile properties (i.e. strength and ductility) for progressively higher Mn additions. Alloying elements that were added to modify binary Ti–Mn alloys primarily included Mo [19], Nb [20], and Zr [21].

Incorporation of Al in Ti alloys is used for a variety of reasons including reducing the cost, decreasing the density, enhance the deformability, improve the oxidation resistance, and increase the mechanical performance via creating a two-phase region. Consequently, Al is the main α stabiliser intentionally added to Ti as it increases the maximum solubility of β stabilisers in the α phase [22]. However, the amount of Al needs to be limited to avoid the embrittlement derived by the precipitation of Ti_3Al intermetallic compound [23,24]. In literature, fewer studies are available on ternary alloys based on the combined addition of Cu and Mn [25,26], Al and Cu [27–30], and Al and Mn [31–34] compared to the binary systems and, to the best knowledge of the authors, no studies considered the development of Ti-based quaternary alloys considering the simultaneous addition of Cu, Mn and Al. Consequently, the aim of this work is to design powder metallurgy quaternary Ti–Cu–Mn–Al alloys to be manufactured via press and sinter to gain understanding of the effect of the alloy composition on their physical properties, microstructural evolution, and resulting mechanical behaviour.

2. Experimental procedure

The design of the quaternary Ti–Cu–Mn–Al alloys was done by means of the molybdenum equivalent parameter (Mo_{eq}), which considers the stabilisation strength of different alloying elements [35,36], as defined by Wang et al. [37]. A short version is reported in Eq. (1):

$$Mo_{eq} = 1.50 \cdot Cu + 2.26 \cdot Mn - 1.47 \cdot Al \quad \text{(Eq. 1)}$$

As per the definition proposed by cotton et al. [38], β-rich α+β titanium alloys have $Mo_{eq} < 5$, near-β titanium alloys have $Mo_{eq} \geq 5$ but lower 10, and metastable β titanium alloys have $Mo_{eq} \geq 10$ but lower 30. A quaternary Ti–Cu–Mn–Al chemical composition was selected for each of those and the details are reported in Table 1. The Cu to Mn ratio was maintained consant and the amount of Al fixed at 2.5 wt.%.

The raw materials for the study were elemental powders available commercially. The hydride-dehydride (HDH) irregular Ti powder (Goodfellow Ltd.) had particle size lower than 75 μm and purity of 99.4 %. The dendritic Cu powder (Merck KGaA) had particle size smaller than 45 μm and 99.7 % purity. The Mn angular powder (Sigma Aldrich Ltd.) had particle size lower than 63 μm and purity greater than 99 %. The spherical Al powder (ECKA Granules) had particle size smaller than 45 μm particle size and >99 % purity. The fabrication process initiated with mixing the raw powders in a V-blender for 30 min with a rotational speed of 30 Hz. A 100-ton hydraulic press was used to produce green compacts with a 40 mm diameter cylindrical shape via cold pressing for 10 s at 600 MPa. Additionally, the walls of the die were lubricated with a graphite coating to reduce friction. To avoid contamination, no lubricant was added to the powders. The green compacts were placed in a vacuum sintering furnace for 2 h at 1300 °C with a heating rate of 10 °C/min and final furnace cooling under vacuum. These conditions were selected from literature on powder metallurgy of Ti alloys [2,39,40].

Table 1
Details of the quaternary Ti–Cu–Mn–Al alloys studied.

Alloy	Ti [wt. %]	Cu [wt. %]	Mn [wt. %]	Al [wt. %]	Mo_{eq}
Ti–1Cu–1Mn-2.5Al	95.5	1	1	2.5	0.1
Ti-3.5Cu-3.5Mn-2.5Al	90.5	3.5	3.5	2.5	9.5
Ti–5Cu–5Mn-2.5Al	87.5	5	5	2.5	15.1

The theoretical density was calculated via the rule of mixture, whereas the Archimedes' principle was used to obtain the sintered density. Before microstructural characterisation, the samples were polished and etched using Kroll reagent (3 ml HF + 6 ml HNO_3 + 91 ml H_2O). Micrographs were captured using an Olympus GX71 light optical microscope and a Philips XL-30 scanning electron microscope. XRD analysis (Cu K_α radiation) was carried out using the following parameters: scanning angle of 30–80°, steep size of 0.013°, voltage of 45V, and current of 40 mA. The tensile properties were obtained from, at least, three dog-bone samples (cross-section of 2 × 2 mm^2, gauge length of 20 mm) per composition. The tests were conducted on a Instron 33R4204 electro-mechanical testing machine with a 0.1 mm/min crosshead speed. The change in elongation was recorded via an extensometer. The Rockwell Hardness method with HRA scale was used to assess the hardness of the samples.

3. Results and discussion

Fig. 1 shows representative micrographs of the quaternary Ti–Cu–Mn–Al alloys where it can be seen that residual porosity is present. Specifically, the volumetric amount of residual pores increases with the alloying elements content and, regardless of the chemical composition, they are isolated and uniformly distributed. This is an indication of the fact that the alloys reached the last stage of sintering upon their manufacturing where homogenisation of the chemistry is complete. However, it can also be seen that the morphology of the porosity changes, switching from purely spherical to more irregular as the amount of eutectoid β stabilisers increases. As the alloys were sintered under the same conditions, this reflects the fact that a progressively higher amount of thermal energy is invested in the diffusion and homogenisation of the alloying elements rather than in the densification of the alloys.

In terms of microstructure, it can be seen that all the quaternary Ti–Cu–Mn–Al alloys are characterised by a lamellar structure typical of Ti alloys bearing both α and β stabilisers. The lamellar microstructure is known to lead to the best compromise between strength and toughness in Ti alloys. This microstructure forms upon slow cooling from the β field on crossing the allotropic phase transformation temperature (i.e. β transus) and it is composed of α+β lamellae enclosed within α grain boundaries or prior β grains. Nonetheless, it can be seen that the overall coarseness of the microstructural features decreases with the amount of eutectoid β stabilisers added or, in turns, for higher Mo_{eq} values. In particular, the size of the prior β grains increases as alloys with higher amount of β stabilisers are sintered at a relatively higher temperature with respect to their β transus, leading to grain growth. Coherently, as more amount of β phase is stabilised within the microstructure, the width of the α lamellae decreases and that of the β lamellae increases resulting in a general refinement. It is also found that a hypoeutectoid substructure is precipitated within the β lamellae for a sufficiently high amount of Cu, which in this instance corresponds to the addition of 3.5 wt.%. This structure is typically found in hypoeutectoid cast binary Ti–Cu alloys [41]. It is worth mentioning that no undissolved powder particles of the alloying elements were found during microstructural analysis, and the homogeneity of the chemical composition is further

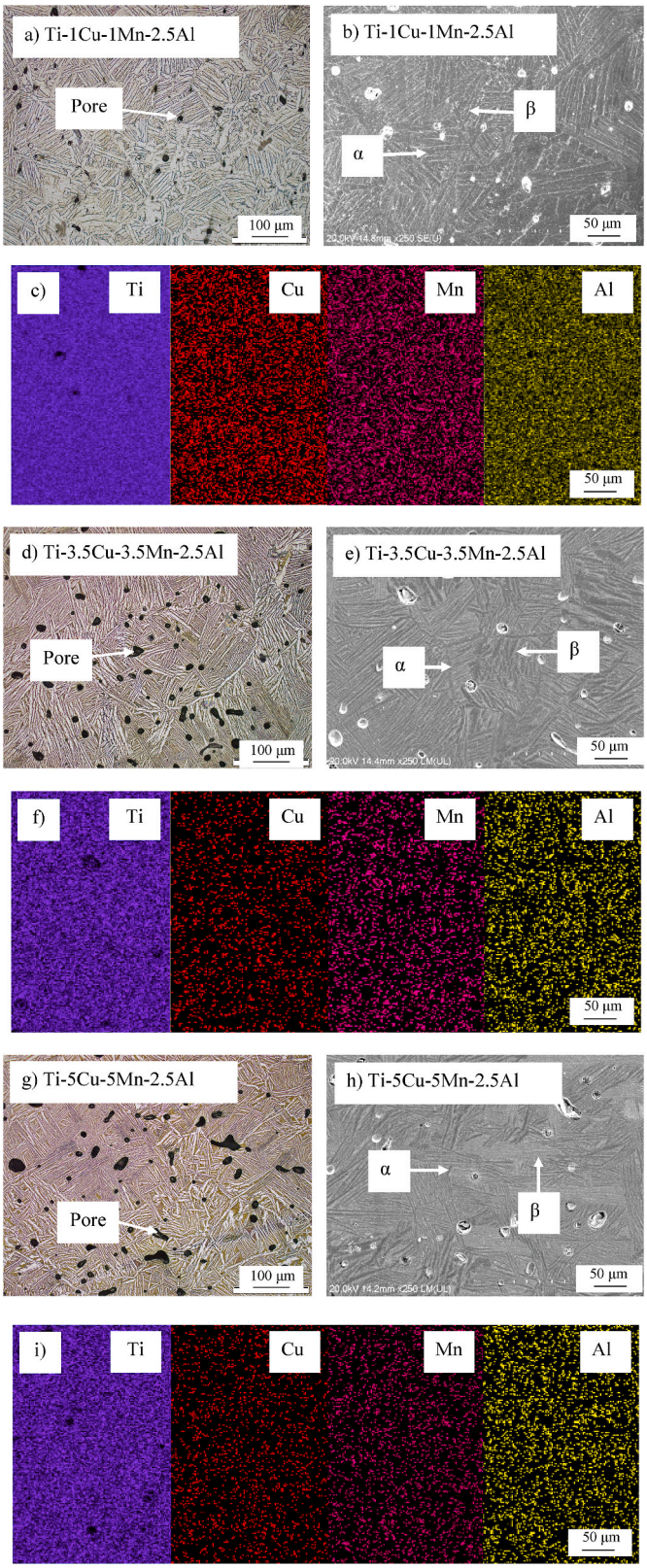

Fig. 1. Representative optical and SEM micrographs and elemental maps, respectively: a-c) Ti–1Cu–1Mn-2.5Al, d-f) Ti-3.5Cu-3.5Mn-2.5Al, and g-i) Ti–5Cu–5Mn-2.5Al.

confirmed by the elemental maps of the distribution of the alloying elements. This could have been expected as the sintering parameters were chosen based on literature about powder metallurgy Ti alloys [18,39,42] and the three alloying elements (namely Cu, Mn and Al) have high diffusion rates in Ti [43]. However, it is worth noticing that the distribution of the alloying elements in the α and β phases is much more homogeneous in the Ti–1Cu–1Mn-2.5Al alloy with respect to the others. For the Ti-3.5Cu-3.5Mn-2.5Al and Ti–5Cu–5Mn-2.5Al alloys, Al is preferentially found in the α phase whereas Cu and Mn in the β phase, coherently with their maximum solubility dictated by the binary phase diagrams [44] and the fact that they are, respectively, α and β stabilisers.

The results of the XRD analysis are illustrated in Fig. 2 where it can be seen that only the equilibrium α phase was detected in the Ti–1Cu–1Mn-2.5Al alloy despite its microstructure being lamellar (Fig. 1a and b). This is due to the fact that the amount of stabilised β phase within the microstructure is below the detection limit of the diffractometer used. In the case of the Ti-3.5Cu-3.5Mn-2.5Al (Fig. 2b), the equilibrium α phase is still the predominant but the main (110) peak of the stabilised β phase and that of the precipitated Ti_2Cu intermetallic phase were also detected, in agreement with the result of the microstructural characterisation. The precipitation of the Ti_2Cu intermetallic phase has been reported in literature to occur for Cu contents of 2 wt.% and above [5]. Similar results are found for the Ti–5Cu–5Mn-2.5Al where several peaks of the stabilised β phase and of the precipitated Ti_2Cu intermetallic phase are present in the XRD pattern (Fig. 2c).

Through the analysis of the relative intensity of the strongest peak of the latter two phases, it is found that both increase with the amount of β stabilisers added or the equivalent Mo_{eq} value (Fig. 2d). However, a linear increase is found for the Ti_2Cu intermetallic phase, which is not the case for the main (110) peak of the stabilised β phase. The overall amount of stabilised β phase still increases when adding 5 wt.% of Cu and Mn, as more peaks related to it are found, which is coherent with microstructural analysis (Fig. 1e and f). Nevertheless, the fact that more Cu is used for the precipitation of the Ti_2Cu intermetallic phase leads to a lower relative intensity of the main (110) peak of the stabilised β phase.

From the variation of the density of the quaternary Ti–Cu–Mn–Al alloys versus their Mo_{eq} value, it can be seen that the green (3.82 → 3.89 g/cm^3), sintered (4.22 → 4.33 g/cm^3), and theoretical (4.54 → 4.83 g/cm^3) density all monotonically increase (Fig. 3a). This is the result of the compromise between the increase of the density induced by the addition of Cu and Mn, which are heavier than Ti, and the reduction of the density brought about by Al, which is lighter. However, from Fig. 3b), it can be seen that the increase in density does not actually translate into a reduction of the porosity. Specifically, it is found that amount of residual pores present in both the green (15.7 → 19.5 %) and sintered (7.1 → 10.3 %) samples linearly increases with the Mo_{eq} value. This means that the addition of the alloying elements powder particles to Ti decreases the compressibility of the powder blend resulting in the decrease of the relative green density. The compressibility of the powder blend is the compromise between the morphology, particle size, and hardness of the different powders. The dendritic and spherical morphology of the Cu and Al powder is detrimental but the angular shape of the Mn powder is favourable. Powders with smaller particle size are generally more difficult to press but the smaller powder particles of the alloying elements can sit in between the gaps left by the coarser Ti powder particles. The low hardness or high deformability of Cu and Al is beneficial but the high hardness of Mn is detrimental to the compressibility.

In terms of relative sintered density, the sintering process generally results in a decrease of the residual porosity content of approximately 9 % due to the effective densification and shrinkage of the alloys during sintering. However, it can be seen that the addition of a greater amount of alloying elements results in a progressively higher amount of residual porosity, in agreement with the results of the microstructural analysis (Fig. 1). It can be also noticed that the gap between the porosity values of the green and sintered density slightly increases (8.7 → 9.1 %) and, consequently, the densification parameter decreases from 55.2 % to

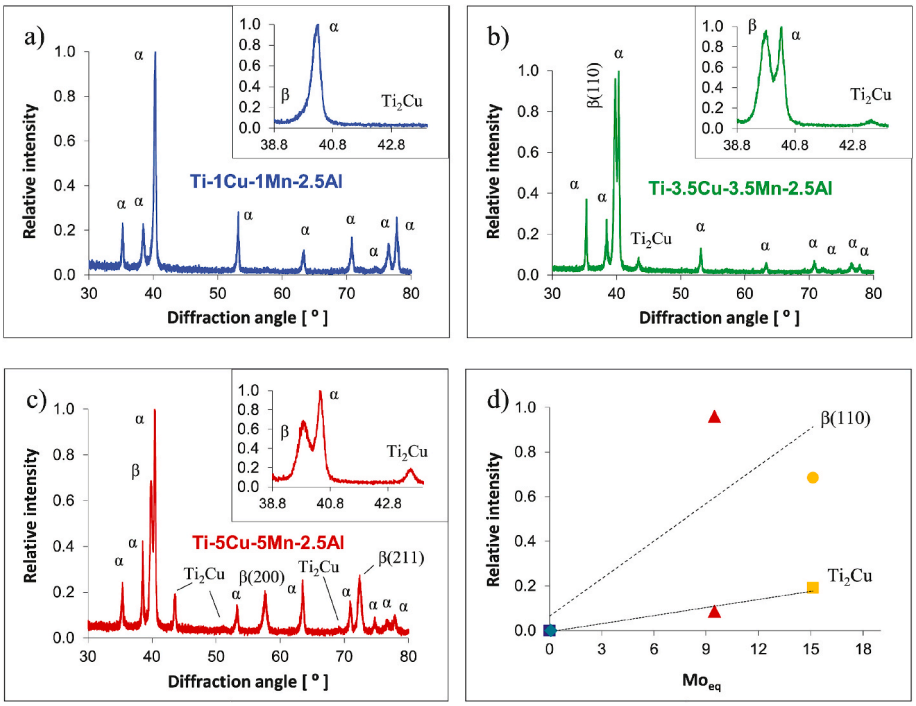

Fig. 2. Results of the XRD analysis of the quaternary Ti–Cu–Mn–Al alloys: a) Ti–1Cu–1Mn-2.5Al, b) Ti-3.5Cu-3.5Mn-2.5Al, c) Ti–5Cu–5Mn-2.5Al, and d) relative intensity of the main β(110) and Ti_2Cu peak as a function of the Mo_{eq} parameter.

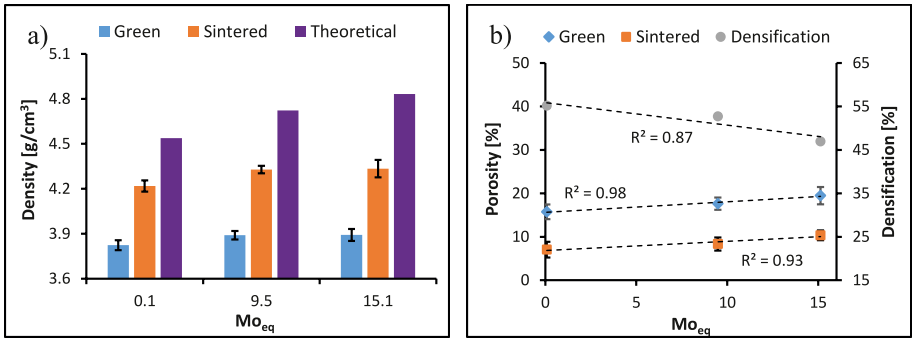

Fig. 3. Variation of the density (a) and of the porosity-densification (b) of the quaternary Ti–Cu–Mn–Al alloys as a function of the Mo_{eq} parameter.

46.9 %. This reinforces the fact that a progressively higher amount of thermal energy is spent in the dissolution of the alloying elements powder particles to achieve a homogenisation of the chemistry rather than on the densification of the alloys. It is worth mentioning that the residual porosity and densification values shown in Fig. 3 for the sintered quaternary Ti–Cu–Mn–Al alloys are comparable to those of other powder metallurgy Ti alloys obtained via the blended elemental approach [18,39,42,45].

Fig. 4 shows typical stress-strain tensile curves of the quaternary Ti–Cu–Mn–Al alloys where it can be seen that, regardless of the chemical composition, each alloy exhibits a ductile behaviour as it undergoes plastic deformation after the initial elastic region. The amount of sustained plastic deformation decreases, and consequently the stress withstood by the alloy increases, for higher additions of β stabilisers making the alloy progressively more brittle. It can also be seen that there is a much more significant loss of ability to withstand plastic deformation when the amount of Cu and Mn is increased to 3.5 wt.% with respect to the further increment to 5 wt.%. This behaviour is consequently reflected on the failure mode and the associated fracture surface of the quaternary Ti–Cu–Mn–Al alloys. Therefore, the fractography micrograph of the Ti–1Cu–1Mn-2.5Al alloy shows a rough surface primarily composed of ductile dimples, plastically deformed residual pores, and intergranular failure along the α grain boundaries (Fig. 4b). This agrees with the good toughness and high deformability of this alloy. The fracture surface of the Ti-3.5Cu-3.5Mn-2.5Al alloy is significantly flatter, a great number of ductile dimples is still present but so are undeformed residual pores. Tear ridges due to the intergranular failure of the α grain boundaries are visible as well as a great number of shallower elevations corresponding to the intergranular failure along the α+β lamellae (Fig. 4c). The fracture surface of the Ti–5Cu–5Mn-2.5Al alloys resembles that of the Ti-3.5Cu-3.5Mn-2.5Al alloy. Primary differences are much shallower tear ridges and intergranular α+β lamellae' elevations as well as fewer and less pronounced ductile dimples resulting in an overall flatter surface typical of more brittle materials (Fig. 4d).

Fig. 5 shows the variation of the average tensile properties including yield stress, ultimate tensile strength, and elongation at failure of the quaternary Ti–Cu–Mn–Al alloys. As expected from the stress-strain tensile curves (Fig. 4), both the yield stress and the ultimate tensile strength increase with the progressive addition of a greater amount of alloying elements. This results in a linear relationship between these properties and the Mo_{eq} parameter. More in detail, the yield stress increases from 632 MPa to 921 MPa and the ultimate tensile strength from

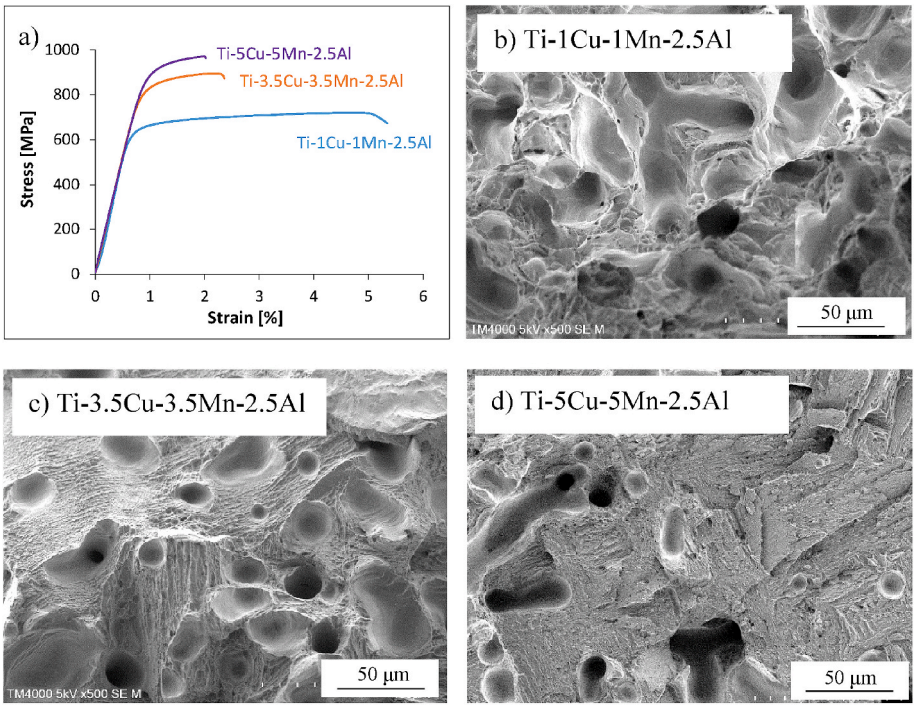

Fig. 4. Typical stress-strain tensile curves (a) and representative results of the fractographic analysis of the quaternary Ti–Cu–Mn–Al alloys: b) Ti–1Cu–1Mn-2.5Al, c) Ti-3.5Cu-3.5Mn-2.5Al, and d) Ti–5Cu–5Mn-2.5Al.

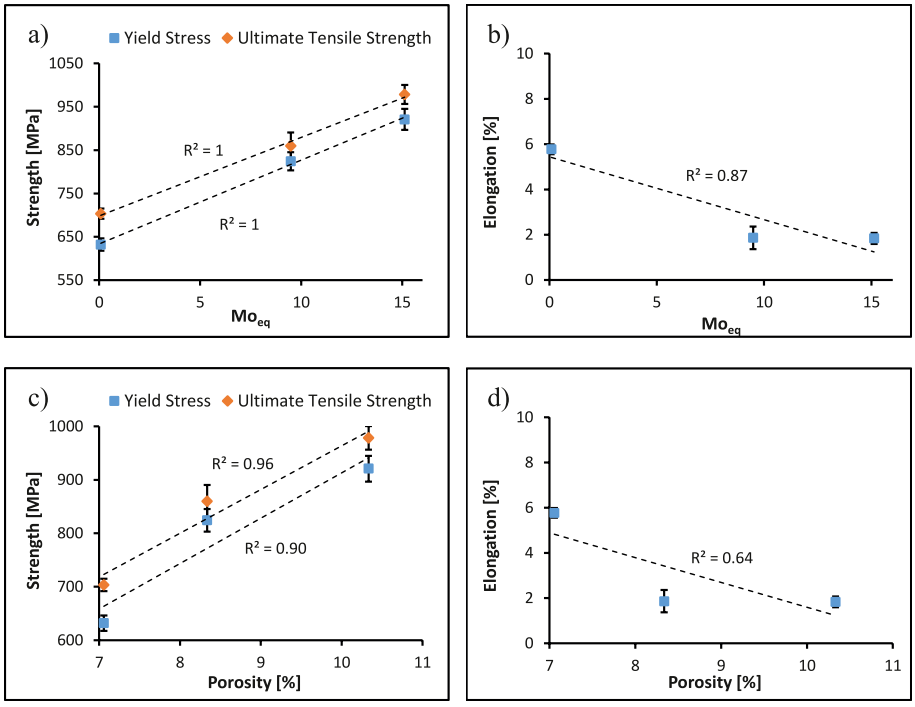

Fig. 5. Average tensile properties of the quaternary Ti–Cu–Mn–Al alloys: a) strength as a function of the Mo_{eq} parameter, b) elongation as a function of the Mo_{eq} parameter, c) strength as a function of porosity, and d) elongation as a function of porosity.

703 MPa to 978 MPa. Strengthening of the quaternary Ti–Cu–Mn–Al alloys concurrently results in the decrease of the elongation at failure from 5.8 % to 1.8 % with the Ti-3.5Cu-3.5Mn-2.5Al alloy having a lower ductility than the expected from a purely monotonic decrement. The described tensile behaviour is the result of the compromise between several aspects sparking from the addition of a progressive higher amount of the alloying elements. Firstly, the addition of greater content of Al, Cu and Mn leads to solid solution strengthening as a larger amount of these atoms substitute Ti atoms in its lattice. The addition of Cu and Mn also results in the stabilisation of a higher amount of β phase, which is stronger than the α phase. Furthermore, a continuous refinement of the microstructural features is obtained as a consequence of the larger amount of stabilised β phase (Fig. 1). Finer microstructures are characterised by a larger amount of grain boundaries [46], especially between

the α+β lamellae, which significantly hinder dislocations movement. For a sufficiently high content of Cu, 3.5 wt.% in this instance, precipitation of the Ti_2Cu intermetallic phase occurs (Fig. 2). The formation of Ti_2Cu particles within the microstructure improves the strength due to dislocation pinning at the grain boundaries [47], where it has been reported that the eutectoid particles present in the α grains of binary Ti–Cu alloys is a leading cause for strength enhancement and low ductility [5]. Lastly, the increase of the Al, Cu and Mn contents also results in the sintered alloy having a greater amount of residual porosity (Fig. 3). The amount, morphology, and overall distribution of the residual pores affect the mechanical behaviour as pores are stress concentration sites, they reduce the effective load bearing cross section, and can provide a preferential path for crack growth.

In the case of the strength, all the aspects (i.e. solid solution, β stabilisation, microstructural refinement, and Ti_2Cu precipitation) with the exception of the increased amount of residual porosity contribute to the strengthening of the quaternary Ti–Cu–Mn–Al alloys. From the analysis of the variation of the strength of the quaternary Ti–Cu–Mn–Al alloys versus the amount of residual porosity (Fig. 5c), it can be seen that a reverse linear trend is achieved where higher amounts of porosity lead to stronger alloys. Therefore, it is concluded that the combined strengthening mechanisms overcome the detrimental effect of the residual pores, justifying the linear increase of the strength with the Mo_{eq} parameter (Fig. 5a). However, from Fig. 5c) it can be seen that the strength of the Ti-3.5Cu-3.5Mn-2.5Al alloy is higher than the expected from a purely linear relationship, which highlights the contribution of the initial precipitation of the Ti_2Cu intermetallic phase in the microstructure of the quaternary Ti–Cu–Mn–Al alloys. Concerning the elongation at fracture, all the strengthening mechanisms as well as the residual pores work against it, resulting in the decreasing trend shown in Fig. 5b). Moreover, a decreasing trend is also found as a function of the amount of porosity (Fig. 5d), which is the expected behaviour. However, it can be seen that the ductility of the Ti-3.5Cu-3.5Mn-2.5Al alloy is lower than the one predicted from a monotonic decrement, which is especially visible in Fig. 5d) and it is due to the formation of the brittle Ti_2Cu intermetallic phase. This permits to highlight two aspects, strengthening of the quaternary Ti–Cu–Mn–Al alloys rather than the amount of porosity actually control the ductility of the alloys, and the residual pores have a remarkably higher impact on the elongation than on the strength of the alloys.

The variation of the hardness of the quaternary Ti–Cu–Mn–Al alloys is shown in Fig. 6 as a function of either the Mo_{eq} parameter or the amount of residual porosity. It can be seen that a linear trend is found in both cases, where the alloys gets harder (58 → 65 HRA) for higher Mo_{eq} values and for greater amounts of porosity present in the microstructure. As for the strength, all the strengthening mechanisms favour a higher hardness whereas porosity detracts from it, where the former are more powerful than the latter. Once again, the effect of the initial precipitation of the Ti_2Cu intermetallic phase is emphasised by the higher hardness of the Ti-3.5Cu-3.5Mn-2.5Al alloy (Fig. 6b).

Fig. 7 shows the strain hardening rate of the quaternary Ti–Cu–Mn–Al alloys as a function of the true plastic strain as well as the true stress versus true strain tensile curves. It is worth mentioning that the strain hardening rate curves of the Ti–5Cu–5Mn-2.5Al alloy could not be properly calculated due to its more brittle behaviour with respect to the other alloys. However, it can be noticed that the position of the strain hardening rate curves reflects the fineness of the microstructure. The finer the microstructure the more shifted to higher true plastic strain values (i.e. towards the right) the strain hardening rate curve is. The Ti–1Cu–1Mn-2.5Al alloy is characterised by a strain hardening rate which asymptotically decreases (i.e. stage II of deformation) upon the initial tensile loading followed by a more gradual decrease as the plastic deformation of the alloy progresses (i.e. stage III) [48]. In the case of the Ti-3.5Cu-3.5Mn-2.5Al alloy, the initial asymptotic part never converts into stage III of deformation due to the fairly brittle nature of the alloy. It can also be seen that the Ti–1Cu–1Mn-2.5Al alloy is the only one able to withstand plastic deformation after the onset of necking, which is identified by the crossing of its strain hardening rate curve with the respective true stress versus true strain tensile curve [49]. This reflects the higher intrinsic toughness of this alloy in comparison to the other quaternary Ti–Cu–Mn–Al alloys and it is due to its coarser lamellar microstructure and the absence of the precipitation of the Ti_2Cu intermetallic phase.

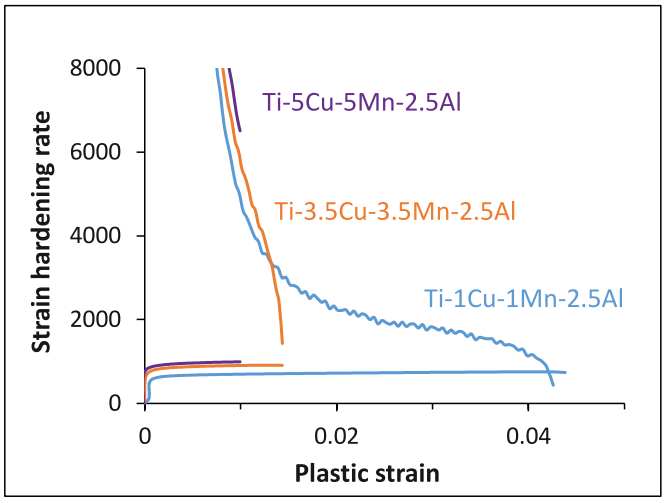

Fig. 7. Strain hardening rate of the quaternary Ti–Cu–Mn–Al alloys as a function of the true plastic strain.

A comparison of the mechanical properties of the quaternary Ti–Cu–Mn–Al alloys with other Cu-, Mn- and Al-bearing Ti alloys primarily obtained via powder metallurgy methods [5,14,18,25,29,32,50,51] including press and sinter and metal injection moulding is reported in Fig. 8. The quaternary Ti–Cu–Mn–Al alloys have slightly better properties than cast binary Ti–Cu alloys, comparable properties with powder metallurgy binary Ti–Mn alloys, powder metallurgy ternary

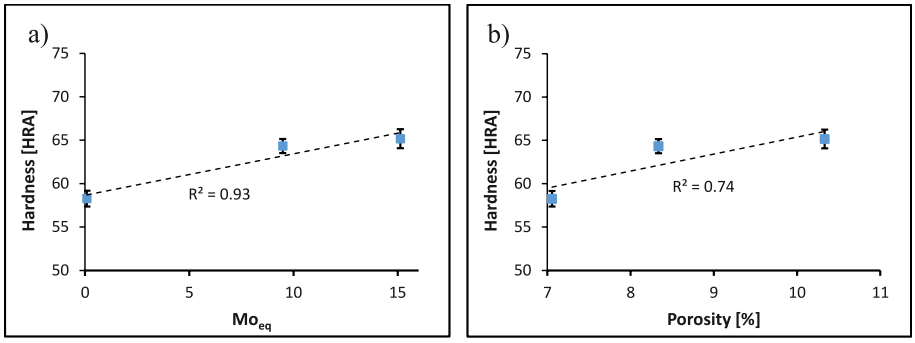

Fig. 6. Variation of the Rockwell hardness of the quaternary Ti–Cu–Mn–Al alloys as a function of the Mo_{eq} parameter (a), and as a function of porosity (b).

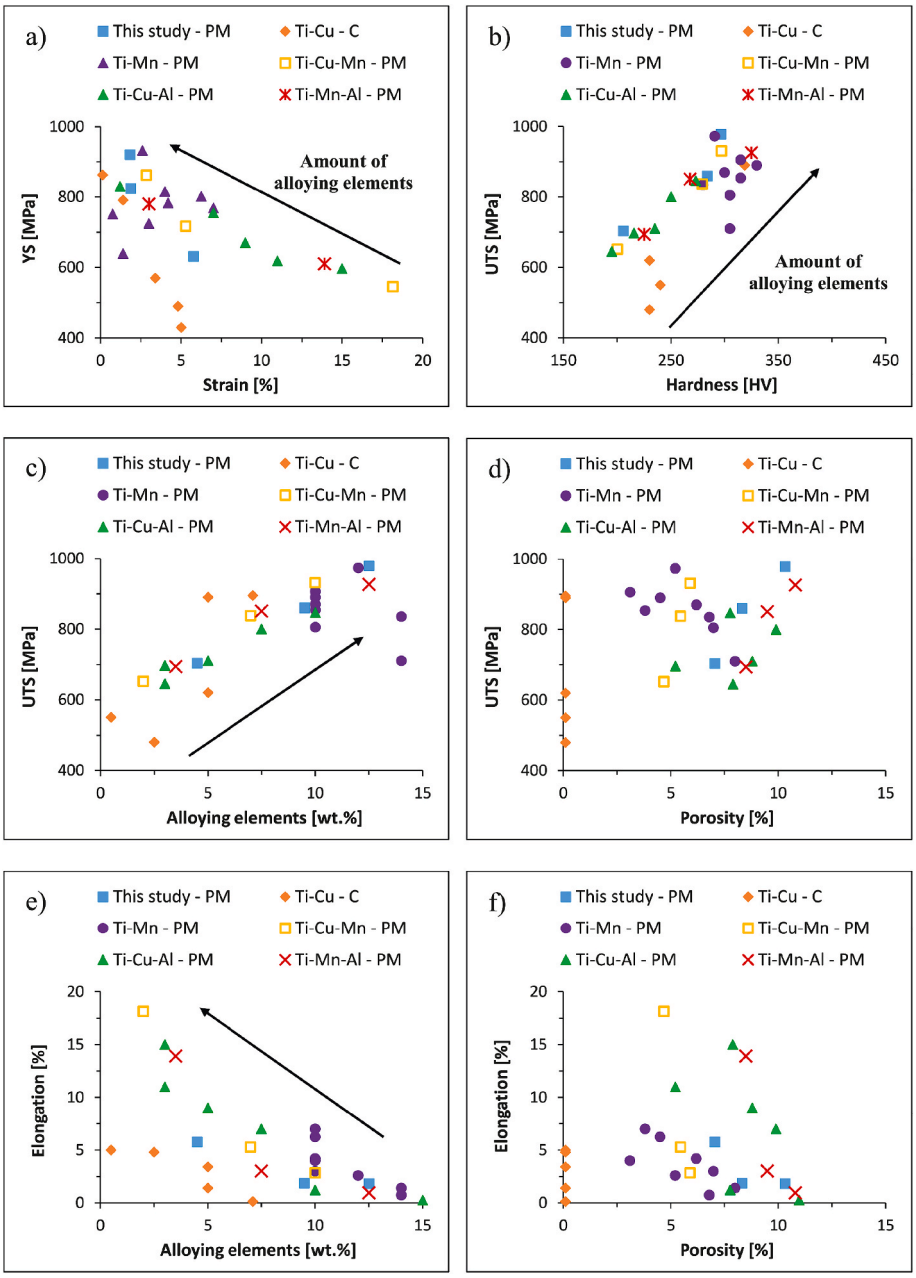

Fig. 8. Comparison of the mechanical properties of the quaternary Ti–Cu–Mn–Al alloys with literature [5,14,18,25,29,32,50,51]: a) yield stress versus elongation at fracture, b) ultimate tensile strength versus hardness, c) ultimate tensile strength versus amount of alloying elements, d) ultimate tensile strength versus porosity, e) elongation at fracture versus amount of alloying elements, and f) elongation at fracture versus porosity.

Ti–Cu–Mn alloys and, generally, higher strength but lower ductility with respect to powder metallurgy ternary Ti–Cu–Al and Ti–Mn–Al alloys (Fig. 8a). However, it is worth mentioning that this comparison is affected by the actual amount of alloying elements present in each alloy as, overall, higher yield stresses but lower elongation values are achieved for progressively greater additions of alloying elements to Ti. From Fig. 8b), it can be seen that the higher the ultimate tensile strength the higher the hardness, which is the expected behaviour. However, the quaternary Ti–Cu–Mn–Al alloys have higher strength but lower hardness in comparison to cast binary Ti–Cu alloys. Moreover, they have higher strength and lower hardness compared to powder metallurgy binary Ti–Mn alloys as well as similar ultimate tensile strength/hardness pairs to powder metallurgy ternary Ti–Cu–Mn, Ti–Cu–Al, and Ti–Mn–Al alloys.

To better understand the effect of the alloy composition on the properties of quaternary Ti–Cu–Mn–Al alloys, their ultimate tensile strength and elongation at fracture is also plotted versus the amount of alloying elements and the amount of residual porosity in Fig. 8. In terms of ultimate tensile strength, for a comparable amount of alloying elements, the quaternary Ti–Cu–Mn–Al alloys have similar strength to that of other Ti alloys, sometimes slightly higher and some other times somewhat lower (Fig. 8c). This is especially noticeable when compared to cast binary Ti–Cu alloys as some alloys with the same chemical composition were heat treated. Furthermore, it can be seen that a higher addition of alloying elements generally leads to a stronger alloy, resulting in an overall increasing linear trend, with the exception of a couple of powder metallurgy binary Ti–Mn alloys. In this case the difference resides in the type of microstructure as a β type microstructure is achieved for a sufficiently high amount of Mn, namely 14 wt.% in this instance. It is worth noticing that no such increasing linear trend is

obtained when the ultimate tensile strength is analysed against the amount of residual porosity (Fig. 8d) as data are much more scattered. This reinforces the finding that the actual microstructural features and the associated strengthening mechanisms are the dominant factor controlling the strength of powder metallurgy Ti alloys rather than their residual porosity. At least at comparable levels of relative sintered density and densification achieved in this study (Fig. 3).

Concerning the elongation at fracture (Fig. 8e), it is found that, for an equivalent total amount of alloying elements, the quaternary Ti–Cu–Mn–Al alloys generally have slightly lower ductility compared to most of the other powder metallurgy Ti alloys considered, but better elongation at fracture with respect to cast binary Ti–Cu alloys. This is a reflection of the effect of different alloying elements as well as the type of manufacturing process used to obtain the alloy as their combination leads to differences in terms of microstructural features. Therefore, an overall decreasing trend of the ductility of the alloys with the total amount of alloying elements is found. Once again, this is not the case of the variation of the elongation at fracture with the amount of residual porosity (Fig. 8f) further confirming the more powerful effect of the microstructural features on the tensile properties of the alloys analysed. It is worth noticing that comparable or better elongation at fracture values are achieved in powder metallurgy Ti alloys with respect to cast binary Ti–Cu alloys despite the fact that that the former are characterised by the presence of residual pores within the microstructure.

4. Conclusions

In this study quaternary Ti–Cu–Mn–Al alloys were designed and manufactured via the powder metallurgy press and sinter method aiming at gaining a better understanding of the effect of the alloy composition on their properties. It is found that the selected quaternary Ti–Cu–Mn–Al alloys are characterised by a lamellar structure, independently of their composition. However, the actual chemistry of the alloy has a remarkable effect on the coarseness of the microstructural features, which become finer for higher Mo_{eq} values due to the greater amount of β phase stabilised within the microstructure. Formation of a hypoeutectoid substructure entailing the precipitation of the Ti_2Cu intermetallic phase is also found for a sufficiently high amount of Cu. The relative amount of the Ti_2Cu intermetallic phase increases as more Cu is added. Residual porosity is also present as microstructural feature, which is typical of powder metallurgy Ti alloys where the final morphology of the pores is affected by the total amount of alloying elements added. This is a reflection of how the thermal energy is distributed between the densification of the alloy and the dissolution of the alloying elements to achieve a homogeneous chemistry. Addition of the elemental powders for the achievement of the desired quaternary Ti–Cu–Mn–Al composition results in the reduction of the powder blend compressibility. The associated reduction of the green density with the amount of alloying elements is directly translated into a decreasing trend of the relative sintered density or increase of the residual porosity. This also affects the densification of the alloys, which thus decreases for greater contents of alloying elements. Independently of the chemistry, the quaternary Ti–Cu–Mn–Al alloys exhibit a ductile behaviour where an increase of the withstood load and a decrease of the elongation is found as the addition of the content of the β stabilising elements increases. This reflects into the switch of the fracture surface from rough and primarily composed of ductile dimples to flat and characterised by intergranular fracture at the α+β lamellae boundaries. The compromise between solid solution strengthening, higher amount of stabilised β phase, refinement of the microstructure, precipitation of the Ti_2Cu intermetallic phase, and increase of the amount of residual porosity leads to stronger and harder but less ductile alloys for higher Mo_{eq} values. The average mechanical properties of the quaternary Ti–Cu–Mn–Al alloys align with the trend found analysing other Cu-, Mn- and Al-bearing Ti alloys manufactured by means of powder metallurgy.

Conflicts of interest or competing interests

The authors declare no conflict of interest.

Data and code availability

All metadata pertaining to this work will be made available on reasonable requests.

CRediT authorship contribution statement

M. Al-hajiri: Methodology, Investigation. **Y. Alshammari:** Methodology, Investigation, Formal analysis. **F. Yang:** Methodology. **L. Bolzoni:** Writing – review & editing, Supervision, Methodology, Investigation, Formal analysis, Conceptualization.

Declaration of competing interest

The authors declare that they have no known competing financial interests or personal relationships that could have appeared to influence the work reported in this paper.

Data availability

Data will be made available on request.

Acknowledgements

This research did not receive any specific grant from funding agencies in the public, commercial, or not-for-profit sectors.

References

[1] B. Bai, E. Zhang, H. Dong, J. Liu, Biocompatibility of antibacterial Ti-Cu sintered alloy: in Vivo bone Response, J. Mater. Sci. Mater. Med. 26 (12) (2015) 265 (12pp.).
[2] M.T. Jia, B. Gabbitas, L. Bolzoni, Evaluation of reactive induction sintering as a manufacturing Route for blended elemental Ti-5Al-2.5Fe alloy, J. Mater. Process. Technol. 255 (2018) 611–620.
[3] R.M. German, Sintering Trajectories: Description on how density, surface Area, and grain size change, JOM 68 (3) (2016) 878–884.
[4] S. Raynova, Y. Collas, F. Yang, L. Bolzoni, Advancement in the pressureless sintering of CP titanium using high-frequency induction heating, Metall. Mater. Trans. 50 (10) (2019) 4732–4742.
[5] M. Kikuchi, Y. Takada, S. Kiyosue, M. Yoda, M. Woldu, Z. Cai, O. Okuno, T. Okabe, Mechanical properties and microstructures of cast Ti-Cu alloys, Dent. Mater. 19 (3) (2003) 174–181.
[6] E. Zhang, X. Wang, M. Chen, B. Hou, Effect of the existing form of Cu element on the mechanical properties, bio-corrosion and antibacterial properties of Ti-Cu alloys for biomedical application, Mater. Sci. Eng. C 69 (2016) 1210–1221.
[7] C.B. Yi, Z.Y. Ke, L. Zhang, J. Tan, Y.H. Jiang, Z.Y. He, Antibacterial Ti-Cu alloy with enhanced mechanical properties as implant applications, Mater. Res. Express 7 (10) (2020) 105404.
[8] E. Zhang, J. Ren, S. Li, L. Yang, G. Qin, Optimization of mechanical properties, biocorrosion properties and antibacterial properties of as-cast Ti-Cu alloys, Biomedical Materials 11 (6) (2016) 065001.
[9] E. Zhang, S. Li, J. Ren, L. Zhang, Y. Han, Effect of extrusion processing on the microstructure, mechanical properties, biocorrosion properties and antibacterial properties of Ti-Cu sintered alloys, Mater. Sci. Eng. C 69 (2016) 760–768.
[10] J. Liu, F. Li, C. Liu, H. Wang, B. Ren, K. Yang, E. Zhang, Effect of Cu content on the antibacterial activity of titanium-copper sintered alloys, Mater. Sci. Eng. C 35 (2014) 392–400.
[11] C. Chaussè de Freitas, K.N. Campo, R. Caram, Thixoforming of titanium: the microstructure and processability of semisolid Ti-Cu-Fe alloys, Vacuum 180 (2020) 109567.
[12] C. Machio, M.N. Mathabathe, A.S. Bolokang, A comparison of the microstructures, thermal and mechanical properties of pressed and sintered Ti-Cu, Ti-Ni and Ti-Cu-Ni alloys intended for dental applications, J. Alloys Compd. 848 (2020) 156494.
[13] M.K. Gouda, K. Nakamura, M.A.H. Gepreel, Effect of Mn-content on the deformation behavior of binary Ti-Mn alloys, Key Eng. Mater. 705 (2016) 214–218.
[14] K. Cho, M. Niinomi, M. Nakai, J. Hieda, P. Fernandes Santos, Y. Itoh, M. Ikeda, Mechanical properties, microstructures, and biocompatibility of low-cost β-type Ti-Mn alloys for biomedical applications, Biomater. Sci.: Processing, Properties and Applications IV 251 (2014) 21–30.

[15] L. Strause, P. Saltman, J. Glowacki, The effect of deficiencies of manganese and copper on osteoinduction and on resorption of bone particles in rats, Calcif. Tissue Int. 41 (3) (1987) 145–150.
[16] H. Sigel, Metal Ions in Biological Systems: Volume 37: Manganese and its Role in Biological Processes Metal Ions in Biological Systems, CRC Press, 2000.
[17] J.-W. Kim, M.-J. Hwang, M.-K. Han, Y.-G. Kim, H.-J. Song, Y.-J. Park, Effect of manganese on the microstructure, mechanical properties and corrosion behavior of titanium alloys, Mater. Chem. Phys. 180 (2016) 341–348.
[18] P. Fernandes Santos, M. Niinomi, H. Liu, K. Cho, M. Nakai, Y. Itoh, T. Narushima, M. Ikeda, Fabrication of low-cost beta-type Ti-Mn alloys for biomedical applications by metal injection molding process and their mechanical properties, J. Mech. Behav. Biomed. Mater. 59 (2016) 497–507.
[19] P. Fernandes Santos, M. Niinomi, H. Liu, K. Cho, M. Nakai, A. Trenggono, S. Champagne, H. Hermawan, T. Narushima, Improvement of microstructure, mechanical and corrosion properties of biomedical Ti-Mn alloys by Mo addition, Mater. Des. 110 (2016) 414–424.
[20] H. Zhang, C. Wang, F. Pyczak, T. Ebel, X. Liu, A new kind of biomedical Ti-Mn-Nb alloy, Phys. Status Solidi 220 (7) (2023) 2200348.
[21] A.H. Awad, M. Abdel-Hady Gepreel, Basic characterization of new Ti-Mn-Zr alloys, Mater. Today: Proc. 33 (2020) 1904–1908.
[22] J. Lu, P. Ge, Y. Zhao, Recent development of effect mechanism of alloying elements in titanium alloy design, Rare Met. Mater. Eng. 43 (4) (2014) 775–779.
[23] A. Gysler, S. Weissmann, Effect of order in Ti3Al particles and of temperature on the deformation behavior of age-hardened Ti-Al alloys, Mater. Sci. Eng. 27 (2) (1977) 181–193.
[24] H. Wu, L. Geng, G. Fan, X. Teng, H. Qi, Nanoscale strain characterization of Ti3Al precipitate-reinforced Ti alloys, Mater. Lett. 209 (2017) 182–184.
[25] L. Bolzoni, M. Alqattan, L. Peters, Y. Alshammari, F. Yang, Ternary Ti alloys functionalised with antibacterial activity, Sci. Rep. 10 (1) (2020) 22201.
[26] M. Alqattan, L. Peters, Y. Alshammari, F. Yang, L. Bolzoni, Antibacterial Ti-Mn-Cu alloys for biomedical applications, Regenerative Biomaterials 8 (1) (2020) rbaa050.
[27] K.Y. Zhu, Y.Q. Zhao, H.L. Qu, Z.L. Wu, X.M. Zhao, Microstructure and properties of burn-resistant Ti-Al-Cu alloys, J. Mater. Sci. 35 (2000) 5609–5612.
[28] M. Koike, T. Okabe, Properties characterization of cast Ti-Al-Cu alloys for dental applications, medical device materials IV, Proceedings from the Materials and Processesfor Medical Devices Conference 2007 (2007) 109–113.
[29] L. Bolzoni, F. Yang, Development of Cu-bearing powder metallurgy Ti alloys for biomedical applications, J. Mech. Behav. Biomed. Mater. 97 (2019) 41–48.
[30] E.-S.M. Sherif, H.S. Abdo, F.H. Latief, N.H. Alharthi, S.Z.E. Abedin, Fabrication of Ti-Al-Cu new alloys by inductive sintering, characterization, and corrosion evaluation, J. Mater. Res. Technol. 8 (5) (2019) 4302–4311.
[31] L. Blacha, B. Oleksiak, A. Smalcerz, T. Matuła, Changes in Ti-Al-Mn alloy compositions during their smelting in a vacuum induction furnace, Archives of Materials Science and Engineering 58 (1) (2012) 28–32.
[32] Y. Alshammari, S. Mendoza, F. Yang, L. Bolzoni, Effect of Mn on the properties of powder metallurgy Ti-2.5Al-xMn alloys, Materials 16 (14) (2023) 4917.
[33] A.V. Mikhaylovskaya, A.O. Mosleh, A.D. Kotov, J.S. Kwame, T. Pourcelot, I. S. Golovin, V.K. Portnoy, Superplastic deformation behaviour and microstructure evolution of near-α Ti-Al-Mn alloy, Materials Science and Engineering: A 708 (2017) 469–477.
[34] K.K. Murthy, S. Sundaresan, Effect of microstructural features on the fracture toughness of a welded alpha-beta Ti-Al-Mn alloy, Eng. Fract. Mech. 58 (1/2) (1997) 29–41.
[35] K. Molchanova, Phase Diagrams of Titanium Alloys, Translation of Atlas Diagram Sostoyaniya Titanovyk Splavov), Israel Program for Scientific Translations, Jerusalem, 1965, p. 154.
[36] B. Tang, Y. Chu, M. Zhang, C. Meng, J. Fan, H. Kou, J. Li, The ω phase transformation during the low temperature aging and low rate heating process of metastable β titanium alloys, Mater. Chem. Phys. 239 (2020) 122125.
[37] Q. Wang, C. Dong, P.K. Liaw, Structural stabilities of β-Ti alloys studied using a new Mo equivalent derived from [β/(α + β)] phase-boundary slopes, Metall. Mater. Trans. 46 (8) (2015) 3440–3447.
[38] J.D. Cotton, R.D. Briggs, R.R. Boyer, S. Tamirisakandala, P. Russo, N. Shchetnikov, J.C. Fanning, State of the art in beta titanium alloys for airframe applications, JOM 67 (6) (2015) 1281–1303.
[39] T. Sjafrizal, A. Dehghan-Manshadi, D. Kent, M. Yan, M.S. Dargusch, Effect of Fe addition on properties of Ti-6Al-xFe manufactured by blended elemental process, J. Mech. Behav. Biomed. Mater. 102 (2020) 103518.
[40] E. Reverte, S.A. Tsipas, E. Gordo, Oxidation and corrosion behavior of new low-cost Ti-7Fe-3Al and Ti-7Fe-5Cr alloys from titanium hydride powders, Metals 10 (21p) (2020) 254.
[41] M. Kikuchi, M. Takahashi, O. Okuno, Mechanical properties and grindability of dental cast Ti-Nb alloys, Dent. Mater. J. 22 (3) (2003) 328–342.
[42] Y. Alshammari, M. Jia, F. Yang, L. Bolzoni, The effect of α+ β forging on the mechanical properties and microstructure of binary titanium alloys produced via a cost-effective powder metallurgy route, Materials Science and Engineering: A 769 (2020) 138496.
[43] A. Amherd Hidalgo, R. Frykholm, T. Ebel, F. Pyczak, Powder metallurgy strategies to improve properties and processing of titanium alloys: a review, Adv. Eng. Mater. 19 (6) (2017) 1600743.
[44] J.L. Murray, in: Phase Diagrams of Binary Titanium Alloys, first ed., ASM International, 1987.
[45] S. Raynova, F. Yang, L. Bolzoni, Mechanical behaviour of induction sintered blended elemental powder metallurgy Ti alloys, Materials Science and Engineering: A 799 (2021) 140157.
[46] L. Bolzoni, N. Hari Babu, Engineering the heterogeneous nuclei in Al-Si alloys for solidification control, Appl. Mater. Today 5 (2016) 255–259.
[47] Y. Xu, J. Jiang, Z. Yang, Q. Zhao, Y. Chen, Y. Zhao, The effect of copper content on the mechanical and tribological properties of hypo-, hyper-and eutectoid Ti-Cu alloys, Materials 13 (15) (2020) 3411.
[48] U.F. Kocks, H. Mecking, Physics and phenomenology of strain hardening: the FCC case, Prog. Mater. Sci. 48 (3) (2003) 171–273.
[49] L. Weber, M. Kouzeli, C. San Marchi, A. Mortensen, On the use of considere's criterion in tensile testing of materials which accumulate internal damage, Scripta Mater. 41 (5) (1999) 549–551.
[50] Y. Alshammari, F. Yang, L. Bolzoni, Fabrication and characterisation of low-cost powder metallurgy Ti-xCu-2.5Al alloys produced for biomedical applications, J. Mech. Behav. Biomed. Mater. 126 (2022) 105022.
[51] A.O.F. Hayama, P.N. Andrade, A. Cremasco, R.J. Contieri, C.R.M. Afonso, R. Caram, Effects of composition and heat treatment on the mechanical behavior of Ti-Cu alloys, Mater. Des. 55 (2014) 1006–1013.